Proceedings of *RAGtime 14–16, 18–22 Sept./15–18 July/11–19 Oct., '12/'13/'14, Opava, Prague, Czech Republic*
Z. Stuchlík, G. Török and T. Pecháček, editors, Silesian University in Opava, 2014, pp. 213–220

Radiating perfect fluid tori in static braneworld spacetime: frequency shift map of torus image

Jan Schee, Pavlína Adámková and Zdeněk Stuchlík

Institute of Physics, Faculty of Philosophy & Science, Silesian University in Opava, Bezručovo nám. 13, CZ-746 01 Opava, Czech Republic

ABSTRACT

The imprints of the tidal-charge parameter b are determined for the spectral line profiles generated by radiation from the surface of optically thick perfect-fluid tori orbiting a spherically symmetric braneworld black holes. We assume that each point on the surface radiates isotropically at a fixed spectral line frequency. We give the direct and indirect image of a torus and the spectral line profile in dependence on the impact parameter for a large inclination angle to the distant observer when the relativistic effects are strongest. We give the map of the frequency shift across the surface and dependence of the maximal and minimal frequency shift of the radiation from the tori surface, giving thus a relevant information on the tidal charge parameter b.

INTRODUCTION

The quantum gravity effects take place in the Planck energy scale where the classical Einstein theory of gravity breaks down. The classical black hole and big bang physical singularities are assumed to be removed by the quantum gravity. However, traces of the quantum gravity effects can be expected even on the energy scales substantially below the Planck scale making the quantum gravity potentially testable. Among many candidates to quantum gravity there are two leading theories, namely the M-theory and the loop quantum gravity. In this paper we consider some effects predicted by the Randall–Sundrum (RS) model that arises from the M-theory (Randall and Sundrum, 1999). The RS model assumes a large scale hidden dimension and can be considered as a practical framework to study possible imprints of the string theory in astrophysical phenomena, using the simple modifications of the standard models of self-gravitating objects like black holes or naked singularities. In the case of the so called braneworld models of black holes the effect of gravity in the hidden dimension is reflected by a single parameter, called tidal charge due to the formal analogy with the electromagnetic effects (Dadhich et al., 2000; Aliev and Gümrükçüoğlu, 2005; Schee and Stuchlík, 2009a,b; Stuchlík and Kotrlová, 2009). The astrophysical phenomena can then put restrictions on the parameters of the braneworld models of black holes.

978-80-7510-127-3

1 STATIC AND SPHERICALLY SYMMETRIC BRANEWORLD BLACK HOLE

In the framework of M-theory (string theory), gravitation is truly higher-dimensional interaction that becomes effectively 4D at energies low enough, $E < E_{\mathrm{Pl}}$. In the braneworld models, the observable universe is a *3-brane* to which the electromagnetic, weak and strong forces (non-gravitational matter fields), described by the standard model, are confined while gravity can enter the extra spatial dimension. The size of such dimension can be much larger than $l_{\mathrm{Pl}} \simeq 10^{-33}$ cm.

Randall and Sundrum (1999) have shown that gravity can be localized near the brane at low energies even in the case of non-compact, infinite size extra spatial dimensions. The corresponding warped spacetimes satisfy 5D Einstein field equations which induce braneworld field equations. The braneworld constrained equations can be given in the form of modified Einstein equations containing additional terms which reflect the bulk effects onto the brane. The vacuum, spherically symmetric solution of the constrained braneworld equations, in the standard Schwarzchild coordinates, reads (Dadhich et al., 2000)

$$\mathrm{d}s^2 = -f(r)\,\mathrm{d}t^2 + \frac{1}{f(r)}\,\mathrm{d}r^2 + r^2\mathrm{d}\theta^2 + r^2\sin^2\theta\,\mathrm{d}\phi^2\,, \tag{1}$$

where the lapse function takes the form

$$f(r) = 1 - \frac{2M}{r} + \frac{\tilde{b}}{r^2} = 1 - \frac{2}{r} + \frac{b}{r^2}\,. \tag{2}$$

Parameter $\tilde{b} \equiv bM^2$ is the braneworld parameter called tidal charge that is reflecting the back reaction of the bulk gravity on the brane. Usually, $b < 0$ is assumed, but $b > 0$ is also considered (see Schee and Stuchlík, 2009a).

The loci of event horizons are given by the condition

$$f(r) = 0\,, \tag{3}$$

which yields

- *two* horizon black hole

$$r_{\mathrm{H}\pm} = 1 \pm \sqrt{1-b} \qquad \text{for } b < 1\,, \tag{4}$$

- one horizon black hole

$$r_{\mathrm{H}} = 2 \qquad \text{for } b = 1\,, \tag{5}$$

- naked singularity for $b > 1$.

2 MOTION OF PHOTONS

The test particle and photon equations of motion are given by the geodesics of the spacetime and in the metric (1) they are separable by Hamilton–Jacobi method. In the case of massless particles (photons) they read

$$\frac{\mathrm{d}r}{\mathrm{d}w} = \pm\sqrt{1 - f(r)\frac{\lambda^2 + q}{r^2}}\,, \tag{6}$$

$$\frac{\mathrm{d}\theta}{\mathrm{d}w} = \pm\frac{1}{r^2}\sqrt{q - \lambda^2\cot^2\theta}\,, \tag{7}$$

$$\frac{\mathrm{d}t}{\mathrm{d}w} = \frac{1}{f(r)}\,, \tag{8}$$

$$\frac{\mathrm{d}\phi}{\mathrm{d}w} = \frac{\lambda}{r^2\sin^2\theta}\,, \tag{9}$$

where we have introduced constants of motion $\lambda = -p_\phi/p_t$ and q reflecting the components of the angular momentum of the particle. In the spherically symmetric spacetimes, the motion occurs always in a central plane of the geometry.

The turning points of the radial motion, if they exists for given constants of motion λ and q, are represented by the roots of the polynomial equation

$$r^2 - f(r)\mathcal{L} = r^4 + \mathcal{L}r^2 - 2\mathcal{L}r + \mathcal{L}b = 0\,. \tag{10}$$

$\mathcal{L} = \lambda^2 + q$ represents the total angular momentum of the particle.

In the case of the latitudinal motion, the turning points occur at

$$\theta = \tan^{-1}\sqrt{\frac{q}{\lambda^2}}\,. \tag{11}$$

3 TEST PERFECT FLUID TORI

The structure and shape of test perfect fluid tori is determined by the relativistic Euler equation. It can be obtained by the following procedure (Kozlowski et al., 1978; Stuchlík et al., 2000):

- The perfect fluid energy-momentum tensor components $T_{\mu\nu}$ relative to coordinate basis read

$$T_{\mu\nu} = (p + \rho)U_\mu U_\nu - p g_{\mu\nu}\,, \tag{12}$$

where p (ρ) is the perfect fluid pressure (energy density) and $g_{\mu\nu}$ are the metric components.
- The elements of the perfect fluid move along circular trajectories, i.e. their four-velocity components read

$$U^\mu = \left(U^t, 0, 0, U^\phi\right)\,. \tag{13}$$

- The Euler equation can be cast as

$$\frac{\nabla_\mu p}{p + \rho} = -\nabla_\mu \ln(U_t) + \frac{\Omega\nabla_\mu l}{1 - \Omega l}\,, \tag{14}$$

where $\Omega(l)$ is the angular velocity (angular momentum) of the fluid element, being defined by

$$\Omega = \frac{U^{\phi}}{U^{t}}, \qquad l = -\frac{U_{\phi}}{U_{t}}. \tag{15}$$

For barotropic fluid ($p = p(\rho)$) it follows from Eq. (14) that there exists an invariant function $\Omega = \Omega(l)$ and surfaces of constant pressure are given by Boyer's condition

$$\int_0^p \frac{\mathrm{d}p}{p+\rho} = W(p) - W(0) = -\ln\frac{U_t}{(U_t)_{\mathrm{in}}} + \int_{l_{\mathrm{in}}}^{l} \frac{\Omega\,\mathrm{d}l}{1-\Omega l}. \tag{16}$$

• To obtain a particular structure, one has to specify the functions $\Omega = \Omega(l)$ and $l = l(r,\theta)$. In the case of a marginally stable torus, the specific angular momentum of the fluid element remains constant across the toroid, $l = l_0 =$ const. The angular velocity of the fluid then reads

$$\Omega = -\frac{g_{tt}}{g_{\phi\phi}} l_0 = \frac{f(r)}{r^2\sin^2\theta} l_0. \tag{17}$$

Under these assumptions, the function $W = W(r,\theta)$ takes the simple form

$$W(r,\theta) = \ln U_t, \tag{18}$$

where U_t follows from normalization of the four-velocity U^{μ}, $-1 = U_{\mu}U^{\mu}$, and reads

$$(U_t)^{-2} = \frac{g_{\phi\phi} + l_0^2 g_{tt}}{g_{tt}g_{\phi\phi}} = \frac{r^2\sin^2\theta - f(r)l_0^2}{f(r)r^2\sin^2\theta}. \tag{19}$$

The final form of the potential given by Eq.(18) reads

$$W(r,\theta) = \frac{1}{2}\ln U_t^2 = \frac{1}{2}\ln\left[\frac{f(r)r^2\sin^2\theta}{r^2\sin^2\theta - f(r)l_0^2}\right]. \tag{20}$$

4 FREQUENCY SHIFT MAP ON THE TORUS IMAGE

In order to illustrate imprints of the braneworld tidal charge parameter b in radiation emitted from the surface of toroidal configurations orbiting the braneworld spherically symmetric black hole, we use several assumptions that simplify the situation to give clear signatures of the tidal charge. We assume the torus to be marginally stable, having $l =$ const, being optically thick, and radiating from the surface where the elements of orbiting torus radiate isotropically and at a frequency fixed across the whole surface. We give the shape and frequency shift map of the radiation from the surface of the torus. Since the frequency of the surface radiation is assumed to be constant, we can construct the profiled spectral lines related to such toroidal configuration. We give also the map of the maximal and minimal frequency shift from the torus surface in dependence on the tidal charge parameter. In our

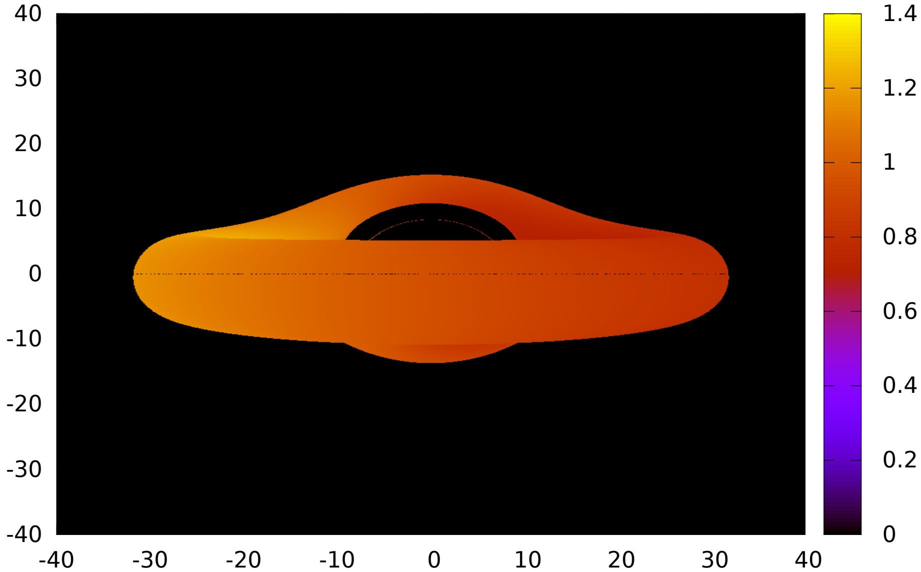

Figure 1. Illustrative example of the torus image and the frequency-shift map. The braneworld parameter is put to $b = -6$ and the observer inclination angle is $\theta_o = 85°$. The colour of the torus depicts the frequency shift labeled by the colour code covering the frequency-shift range $g \in (0, 1.4)$.

calculations we use the techniques developed for the braneworld black hole spacetimes in our previous works (Schee and Stuchlík, 2009a,b; Stuchlík and Kotrlová, 2009).

The frequency shift of the radiation is determined by the formula

$$g = \frac{(k_\mu U^\mu)_{\mathrm{obs}}}{(k_\mu U^\mu)_{\mathrm{em}}} = \frac{\left[f(r) - \Omega r^2 \sin^2\theta\right]^{1/2}}{1 - \lambda\Omega}\,, \tag{21}$$

where λ is the impact parameter of the received photon and Ω is the angular velocity of the radiating element relative to distant observer.

For a series of braneworld parameter b, we have constructed corresponding series of the perfect fluid tori using the following procedure:

- for given braneworld parameter b the Keplerian marginally bound orbit of radius r_{mb} is determined,
- the corresponding angular momentum of the fluid element in the torus is calculated, $l_{\mathrm{torus}} = l_{\mathrm{K}}(r_{\mathrm{mb}}, b)$ where l_{K} is angular momentum of the Keplerian orbit and is given by the formula (Stuchlík and Kotrlová, 2009)

$$l_{\mathrm{K}} = \frac{r^2}{f(r)}\Omega_{\mathrm{K}}\,, \qquad \Omega_{\mathrm{K}} = \sqrt{\frac{r-b}{r^4}}\,, \tag{22}$$

- the value of l_{torus} is used to specify value of the potential W at the torus surface

$$W_{\mathrm{surf}} = hW(r_{\mathrm{AtMin}}, \pi/2; l_{\mathrm{torus}})\,, \tag{23}$$

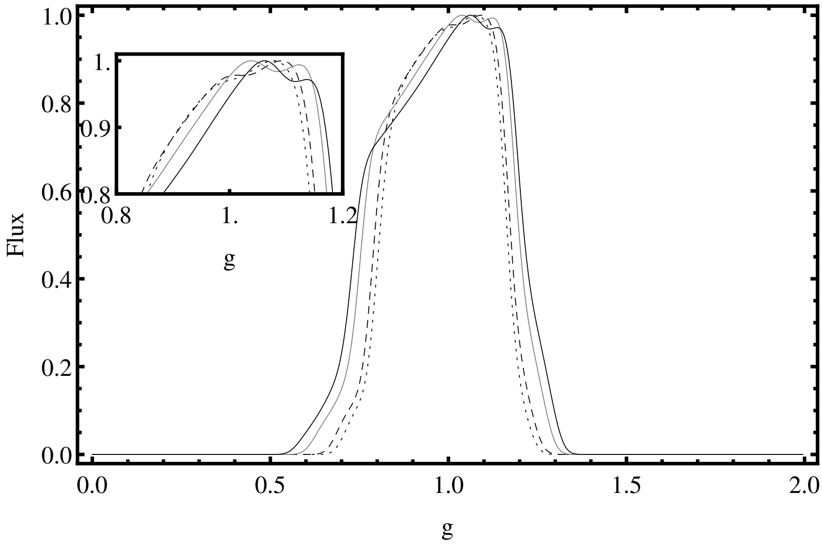

Figure 2. Spectral line profile of radiation from thick tori as detected by observer with inclination $\theta_o = 85°$ generated for four representative values of braneworld parameter $b = -6$ (*dotted*), -4 (*dashed*), -1 (*thin*), and 0 (*thick*).

where we have chosen $h = 0.9$ and $r_{\rm AtMin}$ is the location of the minimum of the potential W, determined from the condition

$$\frac{\mathrm{d}W}{\mathrm{d}r} = 0 \Rightarrow l^2_{\rm torus}\big[b + (r-2)r\big]^2 + (b-r)r^4 = 0\,. \tag{24}$$

Having determined the surface of the marginally stable torus for particular brane-world parameter b, we integrate the equations of motions of photon having impact parameters $(\lambda,\ q)$ corresponding to $(\alpha,\ \beta)$ detector plane coordinates and look for intersection of such null geodesic with the torus surface, $(r_i,\ \theta_i)$; the corresponding frequency shift $g = g(r_i, \theta_i)$ has been calculated from (21) – for details see (Schee and Stuchlík, 2009a,b).

5 RESULTS

As an illustrative example the image of the marginally stable (l = const) torus seen by a distant observer having inclination $\theta_o = 85°$ is shown in Fig. 1. The frequency-shift map is given by the colour varied across the surface of the torus.

Using the methods presented in (Schee and Stuchlík, 2009b), the profiled spectral lines of radiation from whole the torus surface are given in Fig. 2 for some characteristic values of the tidal charge parameter b. We can see that the imprint of the tidal charge is quantitative only, but it is well measurable in principle.

There are minimal, $g_{\rm min}$, and maximal, $g_{\rm max}$, values of the frequency shift of radiation from the torus surface having a fixed frequency. The qualitative and quantitative effect of braneworld parameter is reflected in the plots of the $g_{\rm min}$ ($g_{\rm max}$) values for series values of braneworld parameter b given in Fig. 3.

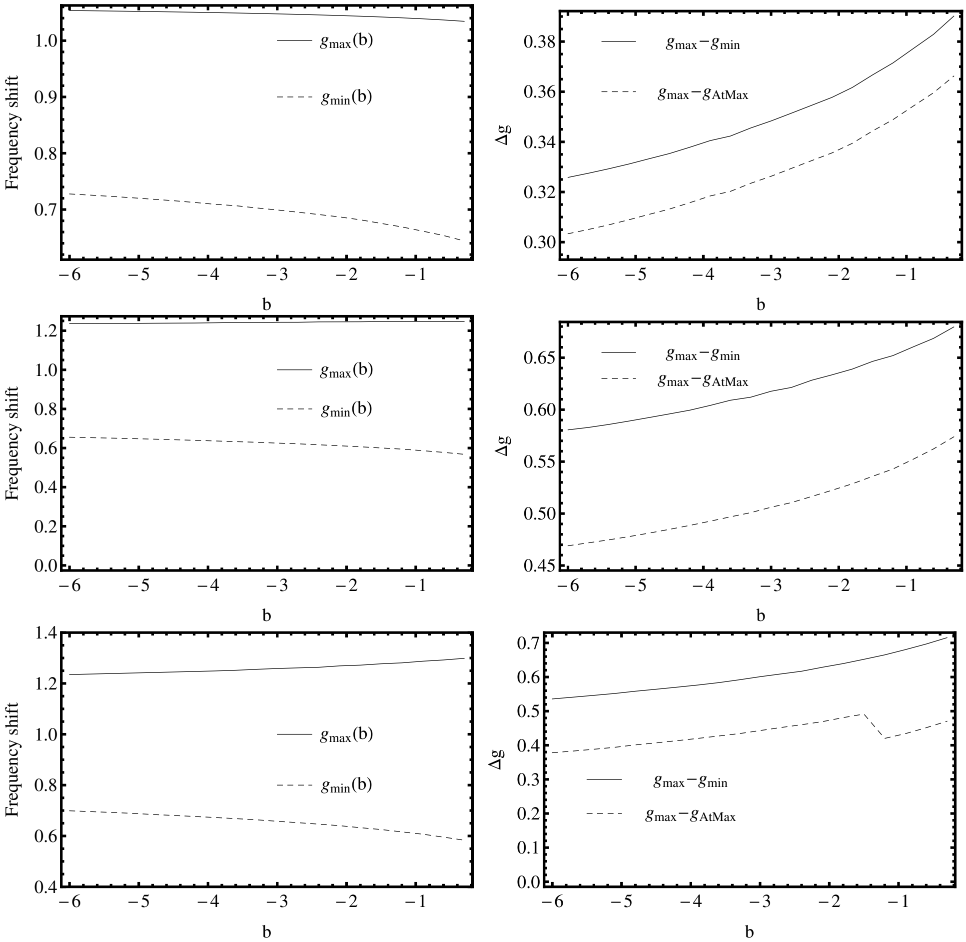

Figure 3. The frequency minimal (maximal) shift $g_{\rm min}$ ($g_{\rm max}$) plotted in the *left* figure and the frequency shift differences $\Delta g(b) = g_{\rm max}(b) - g_{\rm min}(b)$ and $\tilde{\Delta} g = g_{\rm max}(b) - g_{\rm AtMax}(b)$ plotted in the figure on the *right*. The parameter $g_{\rm AtMax}$ is the frequency shift corresponding to maximal specific flux of the profiled line. The observer inclination is $\theta_{\rm o} = 30°$ (*top*), 60° (*middle*) and 85° (*bottom*).

The values of $g_{\rm min}$ and $g_{\rm max}$ determine the width of the profile of spectral line Δg. From the Figure 2 (left column plots and solid lines in the plots in right column), one can conclude that the value of Δg increase with increasing value of braneworld parameter b. So for the case of $b = 0$ the width Δg is largest while for $b = -6$ it reaches the smallest value.

We have defined also a new parameter

$$\tilde{\Delta} g = g_{\rm max}(b) - g_{\rm AtMax}(b) \tag{25}$$

reflecting more subtle character of profiled spectral line. One can see that for small and intermediate inclination angles its behaviour is similar to Δg. However in the case of high inclination angle, $\theta_{\rm o} = 85°$, there is discontinuity in $\tilde{\Delta} g$ reflecting the change of position of the flux maximum, as we vary the value of braneworld parameter. The maximum moves from the right for $b = -6$ to middle for $b = 0$ as one can see also in Fig. 2. To determine how much the choice of the tori sequence influence this effect we shall run another sequences which we postpone to a future work.

6 CONCLUSIONS

We can conclude that the toroidal configuration orbiting in the field of the braneworld black holes can give clear signatures of the influence of the tidal charge parameter of the braneworld. The most useful seem to be the maps of the frequency shift. However, the profiled spectral lines can give a relevant information too.

ACKNOWLEDGEMENTS

The authors would like to thank the internal student grant SGS/23/2013 of the Silesian University, the EU grant Synergy CZ.1.07/2.3.00/20.0071. JS and ZS acknowledge the Albert Einstein Centre for gravitation and astrophysics supported by the Czech Science Foundation Grant No. 14-37086G.

REFERENCES

Aliev, A. N. and Gümrükçüoğlu, A. E. (2005), Charged rotating black holes on a 3-brane, *Phys. Rev. D*, **71**, p. 104027.

Dadhich, N., Maartens, R., Papadopoulos, P. and Rezania, V. (2000), Black holes on the brane, *Phys. Rev. B*, **487**, p. 1.

Kozlowski, M., Jaroszynski, M. and Abramowicz, M. A. (1978), The analytic theory of fluid disks orbiting the kerr black hole, *Astronomy and Astrophysics*, **63**, pp. 209–220.

Randall, L. and Sundrum, R. (1999), An alternative to compactification, *Phys. Rev. Lett.*, **83(23)**, pp. 4690–4693.

Schee, J. and Stuchlík, Z. (2009a), Optical phenomena in the field of braneworld kerr black holes, *Internat. J. Modern Phys. A*, **18**, pp. 983–1024.

Schee, J. and Stuchlík, Z. (2009b), Profiles of emission lines generated by rings orbiting braneworld kerr black holes, *General Relativity and Gravitation*, **41**, pp. 1795–1818.

Stuchlík, Z. and Kotrlová, A. (2009), Orbital resonances in discs around braneworld kerr black holes, *General Relativity and Gravitation*, **41**, pp. 1305–1343.

Stuchlík, Z., Slaný, P. and Hledík, S. (2000), Equilibrium configurations of perfect fluid orbiting schwarzschild-de sitter black holes, *Astronomy and Astrophysics*, **363**, pp. 425–439.